AD-A061 501 TRW INC CLEVELAND OHIO MATERIALS TECHNOLOGY F/G 11/6
EFFECT OF RARE EARTH ADDITIONS ON HYDROGEN EMBRITTLEMENT CRACKI--ETC(U)
OCT 78 A A SHEINKER N00014-74-C-0365
UNCLASSIFIED TRW-ER-7814-4 NL

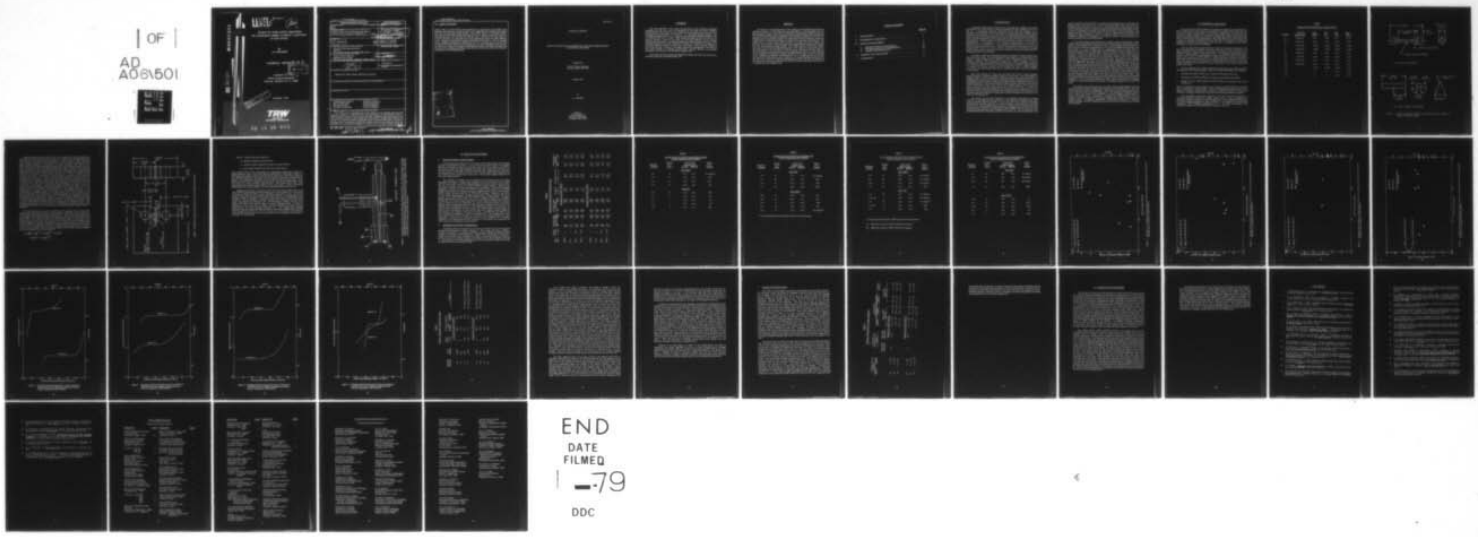

END
DATE FILMED
-79
DDC

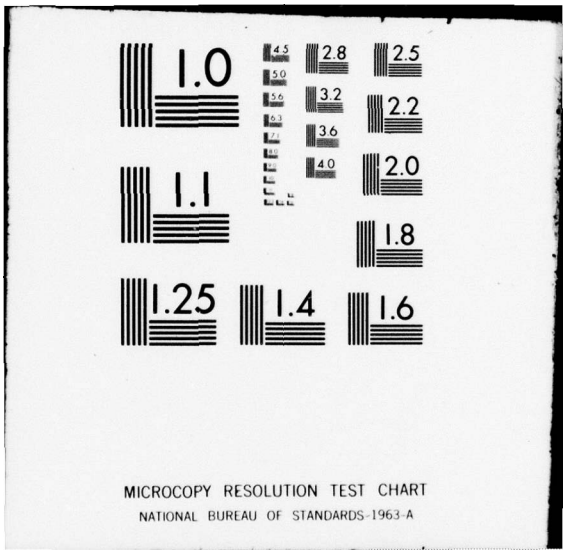
1.0
1.1
1.25
1.4
1.6
1.8
2.0
2.2
2.5
2.8
3.2
3.6
4.0
4.5
5.0
5.6
6.3
MICROCOPY RESOLUTION TEST CHART
NATIONAL BUREAU OF STANDARDS-1963-A

LEVEL II

ER-7814-4

12 sc

TRW INC.

EFFECT OF RARE EARTH ADDITIONS ON HYDROGEN EMBRITTLEMENT CRACKING IN 4340 STEEL

By

A. A. SHEINKER

TECHNICAL REPORT

Prepared for

Office of Naval Research

Contract N00014-74-C-0365

OCTOBER 1978

TRW

EQUIPMENT

MATERIALS TECHNOLOGY

UNCLASSIFIED
SECURITY CLASSIFICATION OF THIS PAGE (When Data Entered)

REPORT DOCUMENTATION PAGE

READ INSTRUCTIONS BEFORE COMPLETING FORM

1. REPORT NUMBER (6)
2. GOVT ACCESSION NO.
3. RECIPIENT'S CATALOG NUMBER (9)

4. TITLE (and Subtitle)
Effect of Rare Earth Additions on Hydrogen Embrittlement Cracking in 4340 Steel (14) TRW-ER-7814-4

5. TYPE OF REPORT & PERIOD COVERED
Technical Rept.
17 June 1977 - 16 June 1978

6. PERFORMING ORG. REPORT NUMBER

7. AUTHOR(s) (10)
A. A. Sheinker

8. CONTRACT OR GRANT NUMBER(s) (15)
N00014-74-C-0365

9. PERFORMING ORGANIZATION NAME AND ADDRESS
Materials Technology Laboratory
TRW Inc.
23555 Euclid Avenue, Cleveland, Ohio 44117

10. PROGRAM ELEMENT, PROJECT, TASK AREA & WORK UNIT NUMBERS

11. CONTROLLING OFFICE NAME AND ADDRESS (11)
Office of Naval Research
Department of the Navy
800 North Quincy Street, Arlington, Virginia 22217

12. REPORT DATE
October 1978

13. NUMBER OF PAGES
41

14. MONITORING AGENCY NAME & ADDRESS (if different from Controlling Office) (12) 45 p.

15. SECURITY CLASS. (of this report)
Unclassified

15a. DECLASSIFICATION/DOWNGRADING SCHEDULE

16. DISTRIBUTION STATEMENT (of this Report)

Approved for public release, distribution unlimited.

17. DISTRIBUTION STATEMENT (of the abstract entered in Block 20, if different from Report)

18. SUPPLEMENTARY NOTES

19. KEY WORDS (Continue on reverse side if necessary and identify by block number)

Hydrogen Embrittlement	Hydrogen Diffusivity
High Strength Steels	Fracture Mechanics
Rare Earth Metals	Crack Propagation
Hydrogen Permeability	Fracture Toughness

20. ABSTRACT (Continue on reverse side if necessary and identify by block number)

The effect of a 0.2 weight percent cerium addition on the hydrogen embrittlement cracking resistance of AISI 4340 steel was investigated at yield strength levels of approximately 210 and 185 ksi (1450 and 1280 MPa). Sustained-load delayed failure data for precracked compact tension specimens electrolytically charged with hydrogen and plated with cadmium exhibited considerable scatter which was attributed to (1) a loss of hydrogen from the specimens during the storage period between cadmium plating and testing and (2) a nonuniform distribution of cerium in the rare earth modified steel. The

DD FORM 1 JAN 73 1473 EDITION OF 1 NOV 65 IS OBSOLETE
S/N 0102-014-6601

UNCLASSIFIED
SECURITY CLASSIFICATION OF THIS PAGE (When Data Entered)

20. Abstract (Continued)

failure time at a given initial stress intensity for a given heat and strength level generally increased with increasing storage time, suggesting that hydrogen had escaped from the test specimens during storage. The cerium content of the delayed failure specimens of the cerium-bearing steels appeared to vary from one specimen to another, also contributing to the the scatter in the test data. Because of the high degree of scatter in this data, no conclusions were drawn regarding the effect of cerium additions on the hydrogen embrittlement cracking resistance of 4340 steel at the two strength levels. Hydrogen permeability measurements on the 0.2 weight percent cerium steel and 4340 steel made without cerium showed that, at a given charging current density, the half-time to reach the steady state hydrogen permeation flux was much longer and the steady state hydrogen permeation flux was three to four times lower in the cerium-bearing steel at both strength levels.

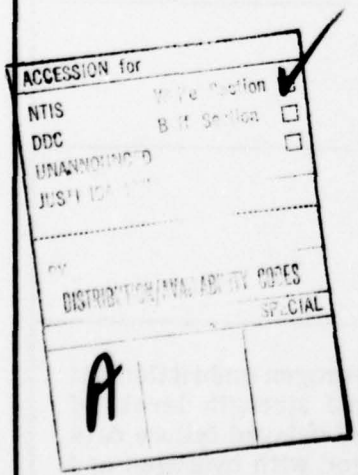

ER 7814-4

TECHNICAL REPORT

EFFECT OF RARE EARTH ADDITIONS ON HYDROGEN EMBRITTLEMENT CRACKING IN 4340 STEEL

Prepared for

Office of Naval Research
Contract N00014-74-C-0365

October 1978

by

A. A. Sheinker

TRW Inc.
TRW Equipment
Materials Technology
Cleveland, Ohio 44117

FOREWORD

The work described in this report was performed in the Materials Technology Laboratory of TRW Inc., under the sponsorship of the Office of Naval Research, Contract N00014-74-C-0365. Dr. P. A. Clarkin acted as Program Monitor for the Navy. The program was administered for TRW by Dr. C. S. Kortovich, Program Manager. The Principal Investigator was Dr. A. A. Sheinker, with technical assistance provided by Mr. J. W. Sweeney and Mr. R. R. Ebert. Work conducted during the first two years of this contract involved a study of the effect of rare earth additions on the hydrogen embrittlement resistance of cathodically charged and cadmium plated 4340 steel. Work conducted during the third year consisted of a study of the effect of rare additions on the stress cracking resistance of 4340 steel in salt water. Work conducted during the fourth and final year, covered in this report, involved an investigation of the effect of rare earth additions on hydrogen embrittlement cracking behavior and hydrogen permeability in 4340 steel at two different strength levels.

This report has been assigned TRW Equipment Number ER 7814-4 and the data are recorded in laboratory notebook Number 794.

ABSTRACT

The effect of a 0.2 weight percent cerium addition on the hydrogen embrittlement cracking resistance of AISI 4340 steel was investigated at yield strength levels of approximately 210 and 185 ksi (1450 and 1280 MPa). Sustained-load delayed failure data for precracked compact tension specimens electrolytically charged with hydrogen and plated with cadmium exhibited considerable scatter which was attributed to (1) a loss of hydrogen from the specimens during the storage period between cadmium plating and testing and (2) a nonuniform distribution of cerium in the rare earth modified steel. The failure time at a given initial stress intensity for a given heat and strength level generally increased with increasing storage time, suggesting that hydrogen had escaped from the test specimens during storage. The cerium content of the delayed failure specimens of the cerium-bearing steels appeared to vary from one specimen to another, also contributing to the the scatter in the test data. Because of the high degree of scatter in this data, no conclusions were drawn regarding the effect of cerium additions on the hydrogen embrittlement cracking resistance of 4340 steel at the two strength levels. Hydrogen permeability measurements on the 0.2 weight percent cerium steel and 4340 steel made without cerium showed that, at a given charging current density, the half-time to reach the steady state hydrogen permeation flux was much longer and the steady state hydrogen permeation flux was three to four times lower in the cerium-bearing steel at both strength levels.

TABLE OF CONTENTS

		Page No.
I	INTRODUCTION	1
II	EXPERIMENTAL PROCEDURE	3
III	RESULTS AND DISCUSSION	10
	A. Mechanical Property Characterization	10
	B. Hydrogen Embrittlement Cracking Results	10
	C. Hydrogen Permeability Results	27
IV	SUMMARY AND CONCLUSIONS	30
V	REFERENCES	31

I INTRODUCTION

Considerable experimental evidence exists indicating that hydrogen can degrade the properties of a wide variety of materials, ranging from high strength steels to soft iron (1). A particularly important observation is the fact that hydrogen can be introduced in a component at any time during its fabrication (casting, welding, surface treatment, heat treatment, etc.) or when used in various applications such as pipelines, containers, gas wells, nuclear reactors, and ships (2). Most of the existing models do not offer a universal explanation for all the phenomenological observations of this hydrogen embrittlement. A factor common to these theories, however, is that in order to obtain embrittlement, it is necessary to have sufficient accumulations of hydrogen at particular sites in the lattice (2). As examples, particular sites can be an internal cavity in the pressure theory (3) or a crack tip in the cohesive energy theory (4,5). This common factor is also the key to current methods aimed at inhibiting hydrogen embrittlement, namely, the prevention of the formation of sufficient accumulations of hydrogen anywhere in a component.

A number of methods of inhibiting hydrogen embrittlement in high strength steels have been under study. These techniques include changes in microstructure (6-8), changes in alloy composition (8), baking (9), surface prestressing (10), plating (11), cathodic protection (12), nonmetallic coating (13), selective changes in surface composition by heat treatment (14), and modification of the embrittling environment (15). Because limitations exist with all of these techniques, research is being conducted to improve the current methods and to develop new ones to inhibit hydrogen embrittlement in high strength steels. One new method is the use of rare earth additions in these alloys.

Rare earth additions to steels have previously been used to control hydrogen blister formation and prevent hydrogen-induced weld cracking. The susceptibility to hydrogen blister or flake formation in 4340-type steels was reduced by adding 0.2 weight percent cerium, which formed stable hydrides below 1850^{o}F (1280^{o}K) (16). The susceptibility of HY-80 steel weldments to hydrogen-induced cracking was decreased by combined additions of cerium and lanthanum (approximately 60 percent cerium and 40 percent lanthanum)at levels of 0.05, 0.09, and 0.13 weight percent, with the maximum effect occurring at the 0.09 weight percent rare earth level (17,18). The addition of approximately 0.2 weight percent Misch metal (50 percent cerium, lanthanum, and small amounts of other rare earths) eliminated the hydrogen typical of that remaining in HY-130 steel weld metal made with an intentional 5 percent hydrogen contamination in the argon arc shielding gas (19).

The effects of rare earth additions on the hydrogen embrittlement cracking resistance of AISI 4340 steel were evaluated at TRW Materials Technology under ONR Contract Number N00014-74-C-0365. In the first phase of this study, the hydrogen embrittlement cracking resistance of vacuum-induction melted 4340 steel containing about 0.05, 0.1, and 0.2 weight percent cerium or lanthanum was determined (20). This material was heat treated to a yield strength level of approximately 205 ksi (1410 MPa) by austenitizing, quenching, and tempering at 450^{o}F (505^{o}K). The test specimens were cathodically charged with hydrogen, plated with cadmium to contain the hydrogen in the

metal, and baked at 300°F (420°K) to homogenize the hydrogen content. Sustained load delayed failure tests showed that, at the 0.2 weight percent rare earth level, the threshold stress intensity (i.e., the stress intensity level below which failure did not occur) increased by a factor of about four and the crack growth rate decreased by about an order of magnitude as compared with 4340 steel without rare earth additions. This improvement was attributed to the ability of the rare earth elements to interact with hydrogen, thereby reducing the supply of hydrogen available for embrittlement and impeding the diffusion of hydrogen to the crack tip where it would accumulate and cause crack growth by local embrittlement.

In the second phase of this program, the concept of rare earth additions to high strength steels was extended to stress corrosion cracking behavior, because this type of failure in high strength steels is believed to be a form of hydrogen embrittlement (21). Three heats of 4340 steel containing zero, 0.20 and 0.30 weight percent cerium were heat treated to a yield strength level of approximately 215 ksi (1480 MPa) by austenitizing, quenching, and tempering at 450°F (505°K), and their resistance to stress corrosion cracking in 3.5 percent sodium chloride solution at room temperature was evaluated. The cerium additions had a much smaller effect on the stress corrosion cracking resistance than the cerium and lanthanum additions had on the hydrogen embrittlement cracking resistance in the previous study. The stress corrosion cracking threshold (K_{Iscc}) was about the same for all three steels, ranging from 15 to 17 ksi $\sqrt{in.}$ (16.5 to 19 MPa $\sqrt{m}$). The higher cerium (0.30%) material had longer failure times and lower average crack growth rates than the lower cerium (0.20%) material. The failure times and average crack growth rates for the steel without cerium could not be directly compared with those for the two cerium-bearing steels because of crack branching which occurred only in the material without cerium. However, it was estimated that in the absence of branching, the failure times for the non-cerium steel would be shorter and the average crack rates higher than those for the lower cerium steel. The difference between the effects of the rare earth additions on stress corrosion cracking and hydrogen embrittlement cracking was attributed to the difference in the source of hydrogen in the two cracking phenomena, which affects the amount of hydrogen available for embrittlement and the processes of hydrogen transport to the tip of the crack.

The purpose of the current study was to develop a better understanding of how the rare earth elements inhibit hydrogen embrittlement in high strength steels. This work represented the final phase of the program. Specifically, efforts were concentrated on cerium additions made to AISI 4340 steel plates. The experimental approach involved first a study of the effects of the additions on internal hydrogen embrittlement at a number of strength levels. Resistance to hydrogen was characterized in terms of delayed failure tests conducted on specimens cathodically charged in sulfuric acid and cadmium plated. In addition, permeability studies were conducted to determine whether hydrogen transport through the steel was affected by the presence of the rare earth additions.

II EXPERIMENTAL PROCEDURE

The test material for this program was obtained by making four experimental 50-pound (23-kg) heats of 4340 steel, two containing 0.20 weight percent cerium and two with no rare earth elements added. The chemical compositions of the four heats are presented in Table 1, along with the specified composition ranges for AISI 4340 steel. All of the standard elements were within the specified ranges, except the silicon in heat X991A, which was just 0.01 percent higher. This slight deviation in silicon content has no effect on hydrogen embrittlement in 4340 steel (22). The presence of 0.02 percent lanthanum in the two cerium-bearing heats was due to its presence in the cerium silicide used to make the cerium additions.

The four heats were vacuum-induction melted and aluminum deoxidized. The cerium was added after deoxidation. The heats were cast in the form of tapered round ingots measuring 4 inches (0.10 m) in diameter at the bottom, 4-3/4 inches (0.12 m) in diameter at the top, and 10 inches (0.25 m) tall. The four ingots were forged in four passes at 2150°F (1450°K), cross-rolled in two passes at 1950°F (1340°K), and straight-rolled in two passes at 1950°F (1340°K). These operations resulted in four plates measuring 3/4 inch (0.019 m) thick, 8-1/2 inches (.22 m) wide, and 20 inches (0.51 m) long. The plates were then annealed at 1150°F (894°K) for 8 hours. This ingot breakdown procedure was indicative of the hot workability of 4340 steel containing 0.20 percent rare earths.

The test specimens were rough machined from the plates, heat treated, and then finish ground to their final dimensions. The heat treatment consisted of the following:

1. Normalize at 1700°F (1200°K) for 15 minutes in salt bath and air cool.

2. Austenitize at 1550°F (1120°K) for 30 minutes in salt bath and oil quench.

3. Temper at either 400°F (480°K) or 750°F (670°K) for 1 hour plus 1 hour in air, and air cool.

Half of the specimens from each plate were tempered at 400°F (480°K) and the other half were tempered at 750°F (670°K). These two tempering temperatures were used to obtain two different strength levels at which to evaluate the effect of rare earth additions on hydrogen embrittlement cracking resistance and hydrogen permeability.

The conventional mechanical properties of the four heats were evaluated by performing duplicate tensile and Charpy impact tests at room temperature on transverse specimens tempered to both strength levels. The dimensions of the tensile and Charpy impact specimens are shown in Figure 1. The hardness of the specimens tempered at 400°F (480°K) was Rockwell C 51 to 52, while the hardness of the specimens tempered at 750°F (670°K) was Rockwell C 43 to 45.

Table I

Compositions of 4340 Steel Heats, Weight Percent

Element	AISI 4340 Specification	Heat X990A	Heat Y30	Heat X991	Heat X991A
C	0.38-0.43	0.39	0.40	0.41	0.39
Mn	0.60-0.80	0.70	0.77	0.70	0.79
P	0.040 max.	0.008	0.009	0.008	0.009
S	0.040 max.	0.008	0.004	0.003	0.004
Si	0.20-0.35	0.26	0.29	0.35	0.36
Ni	1.65-2.00	1.80	1.80	1.80	1.80
Cr	0.70-0.90	0.78	0.79	0.70	0.80
Mo	0.20-0.30	0.25	0.24	0.27	0.26
Al	-	0.053	0.020	0.050	0.07
Ce	-	0	0	0.21	0.20
La	-	0	0	0.02	0.02

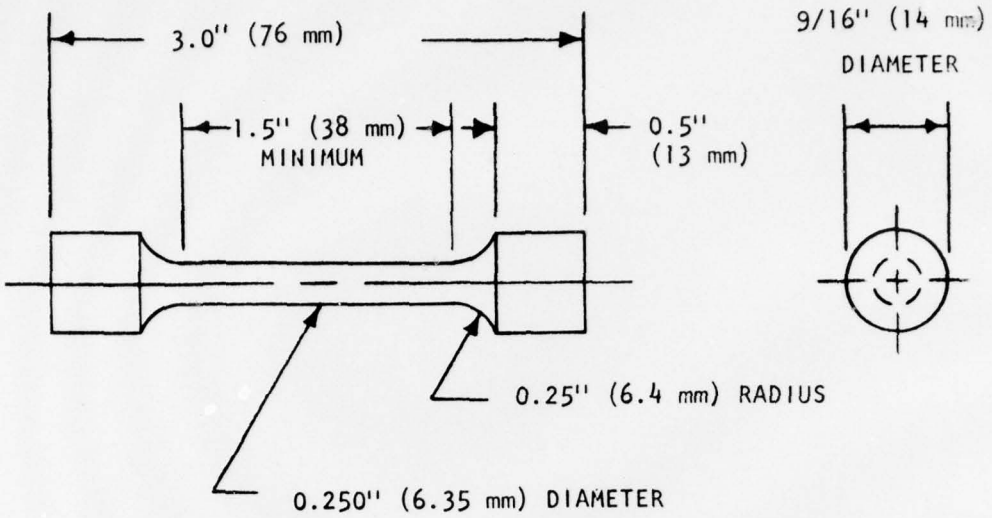

(a) Tensile test specimen.

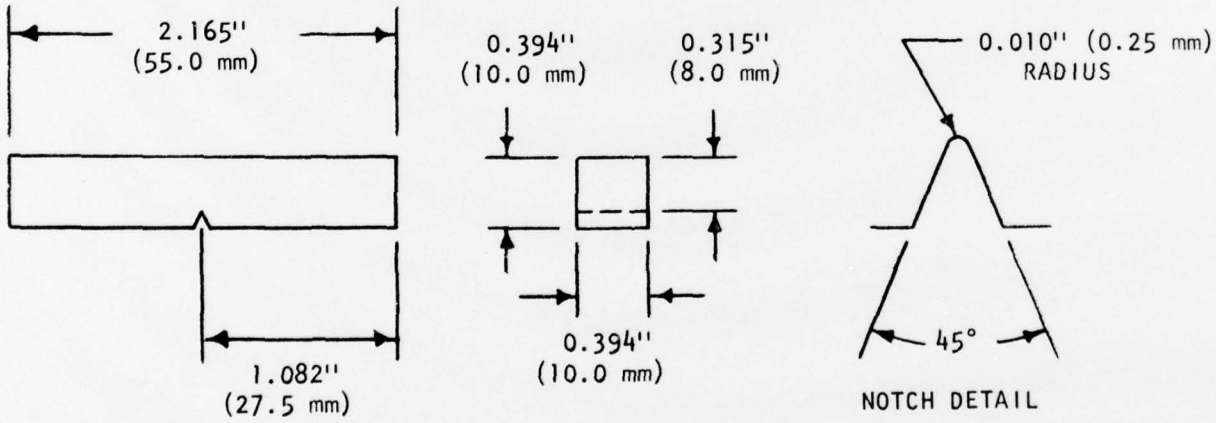

(b) Charpy impact test specimen.

Figure 1. Tensile and Charpy impact test specimens used in mechanical property characterization.

Hydrogen-induced delayed failure tests were conducted at room temperature on precracked compact tension specimens which were charged with hydrogen and plated with cadmium. The design of these specimens is shown in Figure 2. These specimens were cut from the plates in the T-L orientation, i.e., the direction normal to the crack plane (loading direction) was parallel to the width direction of the plate and the direction of expected crack propagation was parallel to the longitudinal direction of the plate. The saw-cut notch was extended 0.050 inch (0.0013 m) by electrical discharge machining (EDM) in order to promote initiation of the fatigue precrack. The specimens were precracked by cyclic tension-tension loading on a Sonntag SF-4 fatigue testing machine at a frequency of 60 hz and a load ratio (R = ratio of minimum load to maximum load) of 0.1. The fatigue cracks were grown to a length of 0.15 inch (0.0038 m) beyond the EDM slot to obtain a total precrack length of 0.58 inch (0.015 m) measured from the load line. These cracks were produced in two successive increments of 0.10 and 0.05 inch (0.0025 and 0.0013 m), with maximum stress intensity factors (K_I) of 20 and 15 ksi $\sqrt{in.}$ (22 and 16.5 MPa $\sqrt{m}$), respectively, at the ends of the two increments of crack growth. This required 19,000 to 44,000 load cycles for the first increment of crack growth and 19,000 to 53,000 load cycles for the second. All of the fatigue cracks grew straight and perpendicular to the loading direction. After precracking, the compact tension specimens were degreased with acetone and electrolytically hydrogen-charged in 4% sulfuric acid at a current density of 0.02 amp./in^2. (30 amp./m^2) for 260 minutes. Following charging, the specimens were rinsed with distilled water and cadmium plated in a sodium cyanide, cadmium oxide bath containing organic brighteners at a current density of 0.14 amp./in^2 (220 amp./m^2) for 15 minutes, to confine the hydrogen within the metal. The specimens were then baked in air at 300°F (420°K) for 60 minutes to homogenize the hydrogen content. This hydrogenating procedure resulted in the type of embrittlement caused by certain metal processing operations and is commonly used in studying hydrogen embrittlement of steels (23).

The delayed failure tests were conducted under sustained load on Satec self-leveling, lever-loaded creep rupture testing machines. These tests were conducted at various initial stress intensity (K_{Ii}) levels to determine failure time as a function of K_{Ii}, the hydrogen embrittlement cracking threshold (K_{th}, the stress intensity level below which failure is not observed), and crack growth rate (da/dt) as a function of the instantaneous stress intensity factor (K_I) for each heat of steel at both strength levels. Fracture toughness (K_{Ic}) tests were performed in accordance with the standard ASTM test procedure (24) on hydrogen-charged and cadmium plated specimens from each heat of steel at both strength levels in order to establish the upper bound of K_I for delayed failure. Stress intensity factors for both the delayed failure and the fracture toughness tests were calculated from the equation (24)

$$K_I = \frac{P}{B\sqrt{W}}\left[29.6\left(\frac{a}{W}\right)^{1/2} - 185.5\left(\frac{a}{W}\right)^{3/2} + 655.7\left(\frac{a}{W}\right)^{5/2} - 1017\left(\frac{a}{W}\right)^{7/2} + 638.9\left(\frac{a}{W}\right)^{9/2}\right]$$

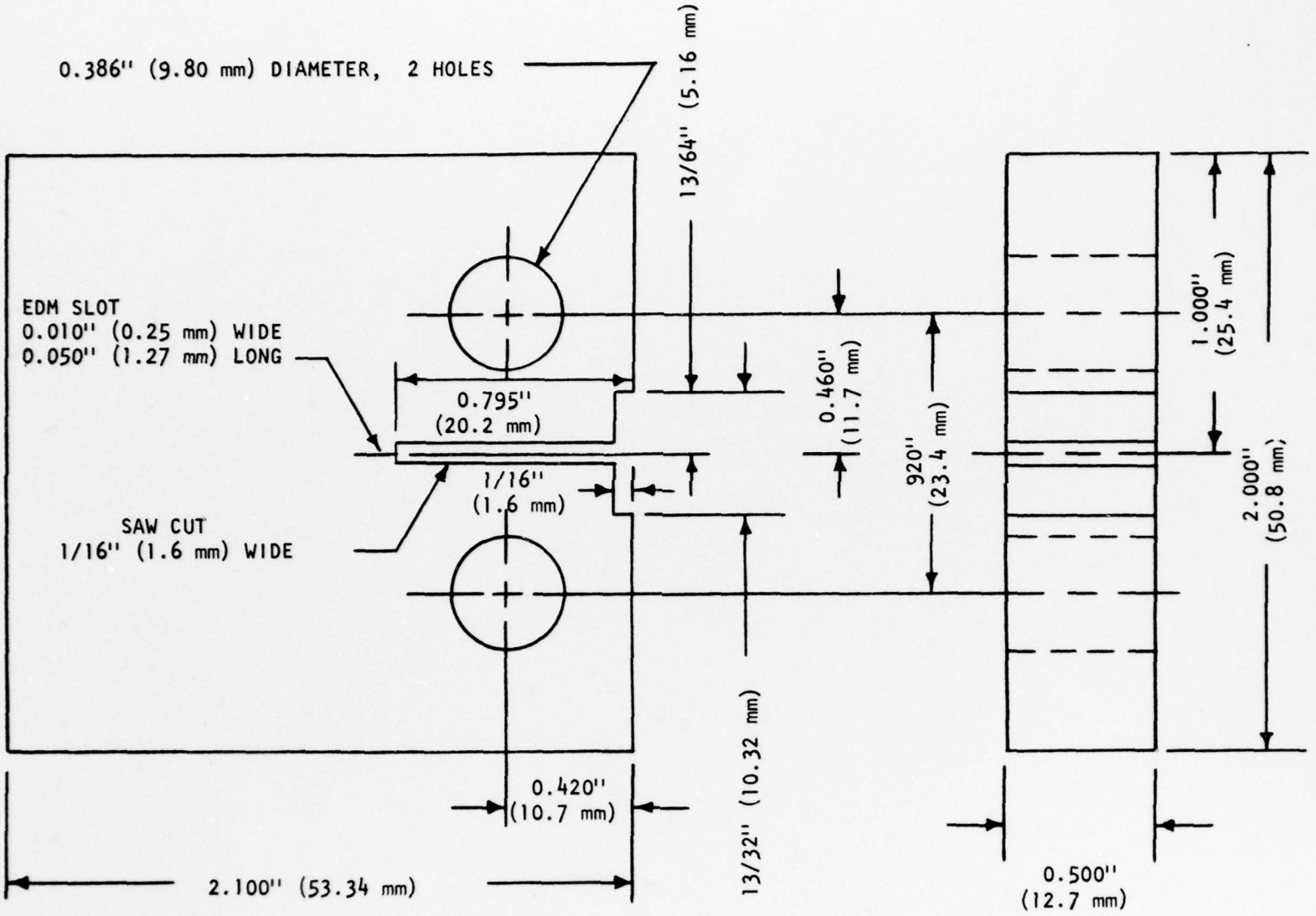

Figure 2. Precracked compact tension specimen used in delayed failure tests.

where P = applied load, pounds (newtons)

B = specimen thickness, inches (meters)

w = specimen width measured from load line, inches (meters)

a = crack length measured from load line, inches (meters)

In the delayed failure tests, crack growth was continuously monitored by means of a double-cantilever clip-on type crack-opening displacement (COD) gage mounted on knife edges spot welded to the front surface of the specimen on each side of the notch. The COD was recorded on a strip-chart recorder and later converted to crack length by means of the compliance relationship for the compact tension specimens (25). Crack growth rate (da/dt) was obtained by calculating the slope of the crack length versus time curve at a series of points along the curve. The delayed failure tests were discontinued after 10,000 minutes if failure did not occur sooner. A total of 10 delayed failure tests, five at each strength level, were performed for each heat of steel.

Hydrogen permeability measurements were made from heats X990A (0% Ce) and X991 (0.21% Ce) heat treated to both strength levels. These samples were 1-inch (0.025 m) square by 0.040-inch (0.001 m) thick membranes which were cut from the 3/4-inch (0.019 m) thick plates and finish ground after heat treatment. The measurements were conducted under the direction of Professor Howard Pickering at Pennsylvania State University. The permeability of hydrogen through these membranes was determined using a Devanathan and Stachurski cell (26) containing a charging solution of 1N sulfuric acid with 20 ppm arsenic added to promote hydrogen entry. A schematic illustration of the cell is shown in Figure 3 and the experimental procedures for the measurements have been detailed previously (27). The steady state hydrogen permeation flux was measured galvanostatically at successive charging current densities of 65, 32, and 9.7 mA/in^2 (1×10^5, 5×10^4, and 1.5×10^4 mA/m^2), and the time to reach one-half of the steady state flux was obtained for the charging current density of 65 mA/in^2 (1×10^5 mA/m^2).

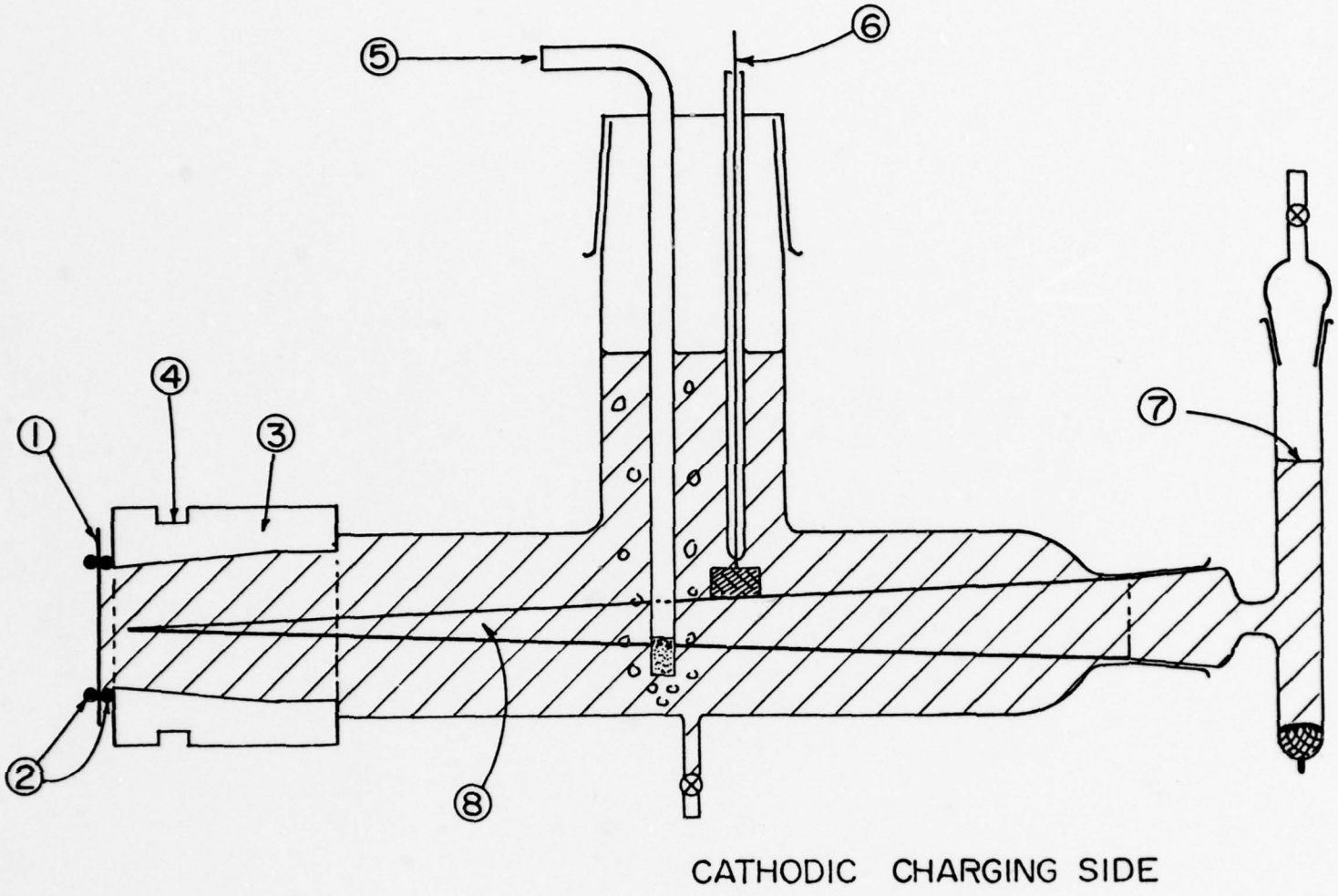

Figure 3. Schematic of one-half of the Devanathan-Stachurski cell (26). (1) Steel membrane, (2) o-rings, (3) plexiglass head, (4) groove for a holder, (5) inlet for pre-purified nitrogen to a gas disperser, (6) Pt auxiliary electrode, (7) Hg/HgO reference electrode, (8) Luggin capillary. The other side of the cell is in a mirror image of the side shown.

III RESULTS AND DISCUSSION

A. Mechanical Property Characterization

The mechanical properties of the four heats of 4340 steel for the two tempering conditions are presented in Table 2. As in the previous studies (20,21), the strength, ductility, and impact resistance all decreased when cerium was added to the steel in both temper conditions. Only transverse specimens were tested, since previous work (21) had shown no significant differences between the longitudinal and transverse mechanical properties of 4340 steel made with or without cerium and processed in the same manner as the material used in this study. This isotropy probably resulted from the cross-rolling operation.

The reductions in strength with the addition of 0.2 percent cerium were small. The largest decrease in average yield strength was only 2.2 percent for the 400°F (480°K) temper condition, and the largest decrease in average ultimate tensile strength was only 3.3 percent, also for the 400°F (480°K) temper condition. However, the reductions in ductility and impact resistance were considerable. The average elongation decreased 41 percent for the 400°F (480°K) temper and 40 percent for the 750°F (670°K) temper, while the average reduction of area decreased 57 percent for the 400°F (480°K) temper and 50 percent for the 750°F (680°K) temper. Except for heat X991A in both temper conditions, the average Charpy impact energy decreased 38 and 56 percent for the 400°F (480°K) and 750°F (670°K) tempers, respectively. The higher Charpy impact values for heat X991A were due to a difference in specimen orientation. Whereas all of the Charpy impact specimens from the other three heats were machined from the plates in the *T-L orientation, i.e., with the direction normal to the notch* (applied stress direction) parallel to the width direction of the plate and the direction of expected crack propagation parallel to the longitudinal direction of the plate, the Charpy impact specimens from heat X991A were inadvertently machined from the plates in the T-S orientation. In this case the direction of expected crack propagation was parallel to the thickness direction of the plate. Consequently, the cracks in the latter specimens propagated in a direction perpendicular to the elongated rare earth oxide inclusions (21), which resulted in an increase in the energy required for crack propagation. Because of the plate-like shape of these inclusions, the mechanical properties in the longitudinal and long transverse (T-L) directions were equal but the short transverse (T-S) properties were different.

B. Hydrogen Embrittlement Cracking Results

The delayed failure test results for the four heats of 4340 steel in the two temper conditions are presented in Tables 3 through 6. The storage time given in Tables 3 through 6 represents the timeelapsed between cadmium plating and delayed failure testing of the compact tension specimens. Failure times are plotted as a function of initial stress intensity (K_{Ii}) in Figures 4 through 7, and crack growth rate (da/dt) is plotted as a function of instantaneous stress intensity factor (K_I) in Figures 8 through 11. The results of the fracture toughness tests used to establish the upper bound of K_I for delayed failure are presented in Table 7.

Table 2

Mechanical Properties of 4340 Steel Heats

Heat No.	Cerium Content %	Yield Strength at 0.2% Offset ksi	Yield Strength at 0.2% Offset MPa	Ultimate Tensile Strength ksi	Ultimate Tensile Strength MPa	Elongation %	Reduction of Area %	Charpy Impact Energy ft-lb	Charpy Impact Energy J
				Tempered at 400°F (480°K)					
X990A	0	210	1450	274	1890	14.0	47.0	14.5	19.7
		208	1430	273	1880	15.0	48.2	15.5	21.0
Y30	0	211	1450	274	1890	14.0	46.9	14.5	19.7
		213	1470	270	1860	8.0	22.9	14.0	19.0
X991	0.21	207	1430	258	1780	3.0	6.7	8.5	11.5
		203	1400	266	1830	10.0	28.4	9.5	12.9
X991A	0.20	208	1430	266	1830	7.0	12.0	28.0	38.0
		205	1410	265	1830	10.5	23.6	36.5	49.5
				Tempered at 750°F (670°K)					
X990A	0	185	1280	207	1430	14.0	52.1	18.0	24.4
		183	1260	207	1430	14.0	51.1	17.5	23.7
Y30	0	188	1300	210	1450	13.5	50.1	17.5	23.7
		187	1290	209	1440	15.0	52.5	18.0	24.4
X991	0.21	180	1240	201	1390	4.0	7.8	8.0	10.8
		186	1280	207	1430	10.5	32.4	7.5	10.2
X991A	0.20	182	1250	204	1410	9.0	30.1	17.0	23.0
		183	1260	204	1410	10.0	32.0	27.5	37.3

Table 3

Delayed Failure Test Results for 4340 Steel Without Cerium Tempered at 400°F (480°F)

Specimen Number	Storage Time Days	Initial Stress Intensity (K_{Ii}) ksi $\sqrt{in.}$	Initial Stress Intensity (K_{Ii}) MPa $\sqrt{m}$	Failure Time Minutes
		Heat X990A		
5-9	13	15.1	16.6	(No failure)
5-7	11	20.3	22.3	366
5-5	12	40.5	44.5	1512
5-3	21	60.5	66.5	720
		Heat Y30		
7-11	16	18.2	20.0	582
7-9	7	18.1	19.9	372
7-7	1	17.9	19.7	60
7-5	1	29.7	32.6	78
7-3	8	49.6	54.5	600

Table 4

Delayed Failure Test Results for 4340 Steel with 0.2% Ce Tempered at 400°F (480°K)

Specimen Number	Storage Time Days	Initial Stress Intensity (K_{Ii}) ksi $\sqrt{in.}$	Initial Stress Intensity (K_{Ii}) MPa $\sqrt{m}$	Failure Time Minutes
		Heat X991		
1-9	28	14.5	16.0	(no failure)
1-7	24	19.8	21.7	6234
1-5	13	39.4	43.3	468
1-3	25	58.8	64.6	8790
		Heat X991A		
6-11	15	18.0	19.8	216
6-9	29	29.8	32.7	5712
6-5	4	29.9	32.9	348
6-7	10	29.6	32.6	162
6-3	11	51.4	56.5	(no failure)*

* Test was discontinued after 28,830 minutes with crack growing.

Table 5

Delayed Failure Test Results for 4340 Steel Without Cerium Tempered at 750°F (670°K)

Specimen Number	Storage Time Days	Initial Stress Intensity (K_{Ii}) ksi $\sqrt{in.}$	Initial Stress Intensity (K_{Ii}) MPa $\sqrt{m}$	Failure Time Minutes
		Heat X990A		
5-6	23	39.6	43.5	(no failure)
5-8	49	50.6	55.6	(no failure)
5-10	51	54.6	60.0	(no failure)
5-4	27	59.4	65.3	1944
		Heat Y30		
7-8	35	54.1	59.5	(no failure)
7-12 (a)	8	58.8	64.6	(no failure)
7-6	30	59.8	65.7	(no failure)*
7-2 (b)	2	59.0	64.8	8766
7-4	3	60.6	66.6	288

* Test was discontinued after 20,000 minutes with crack growing.

(a) Baked for 112 hours at 300°F (420°K) after plating.

(b) Baked for 10 hours at 300°F (420°K) after plating.

Table 6

Delayed Failure Test Results for 4340 Steel With 0.2% Ce Tempered at 750°F (670°K)

Specimen Number	Storage Time Days	Initial Stress Intensity (K_{Ii}) ksi $\sqrt{in.}$	Initial Stress Intensity (K_{Ii}) MPa $\sqrt{m}$	Failure Time Minutes
		Heat X991		
1-6	64	39.8	43.8	(no failure)
1-8	50	49.7	54.6	(no failure)
1-10	53	54.3	59.6	(no failure)
1-4	74	58.8	64.6	3882
		Heat X991A		
6-12	14	50.0	54.9	66
6-8	32	56.0	61.5	2994
6-10	31	55.3	60.7	1122
6-6	0	54.8	60.3	36
6-4	8	59.0	64.9	1044

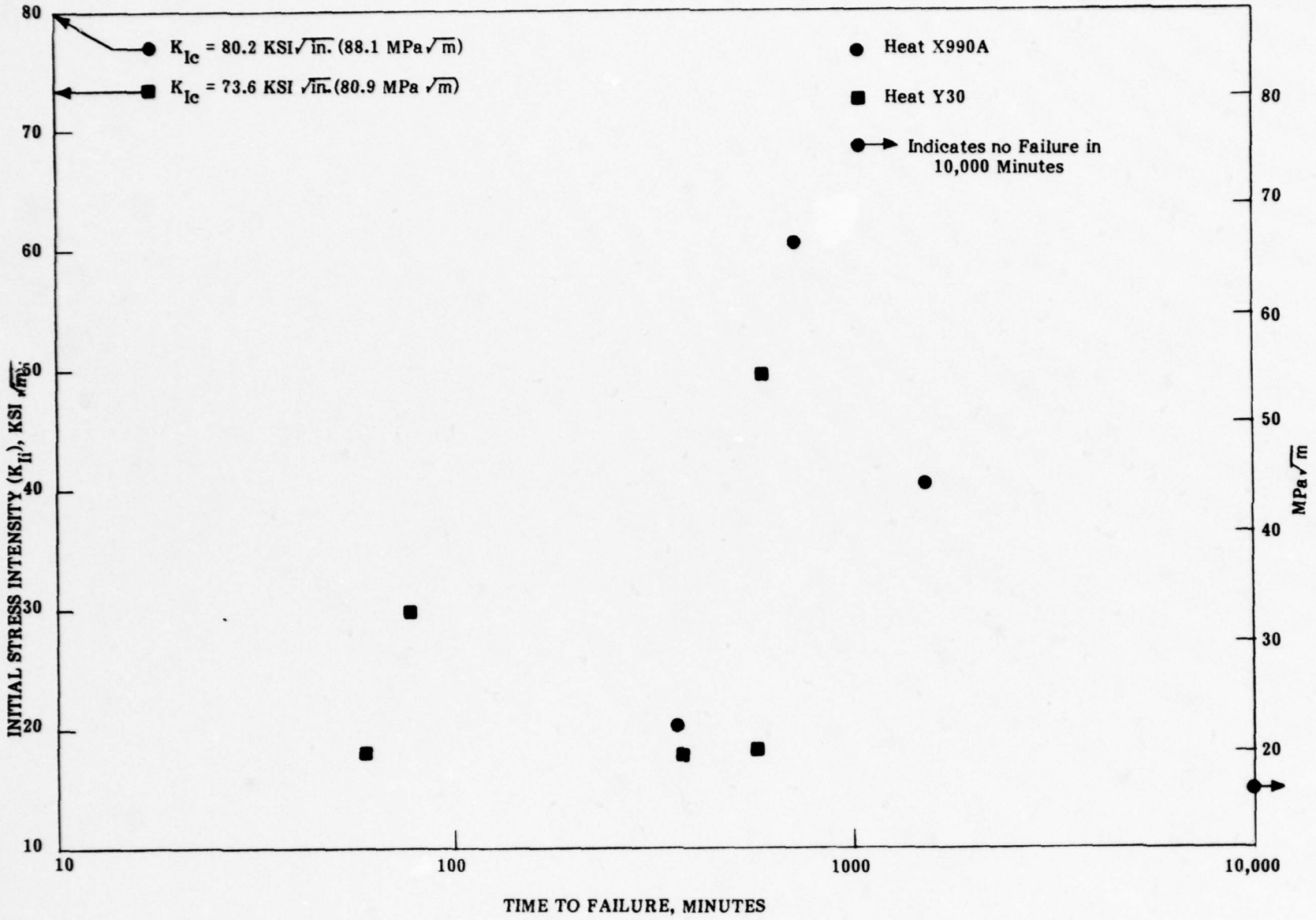

Figure 4. Hydrogen-induced delayed failure time as a function of initial stress intensity for 4340 steel without cerium, tempered at 400°F (480°K).

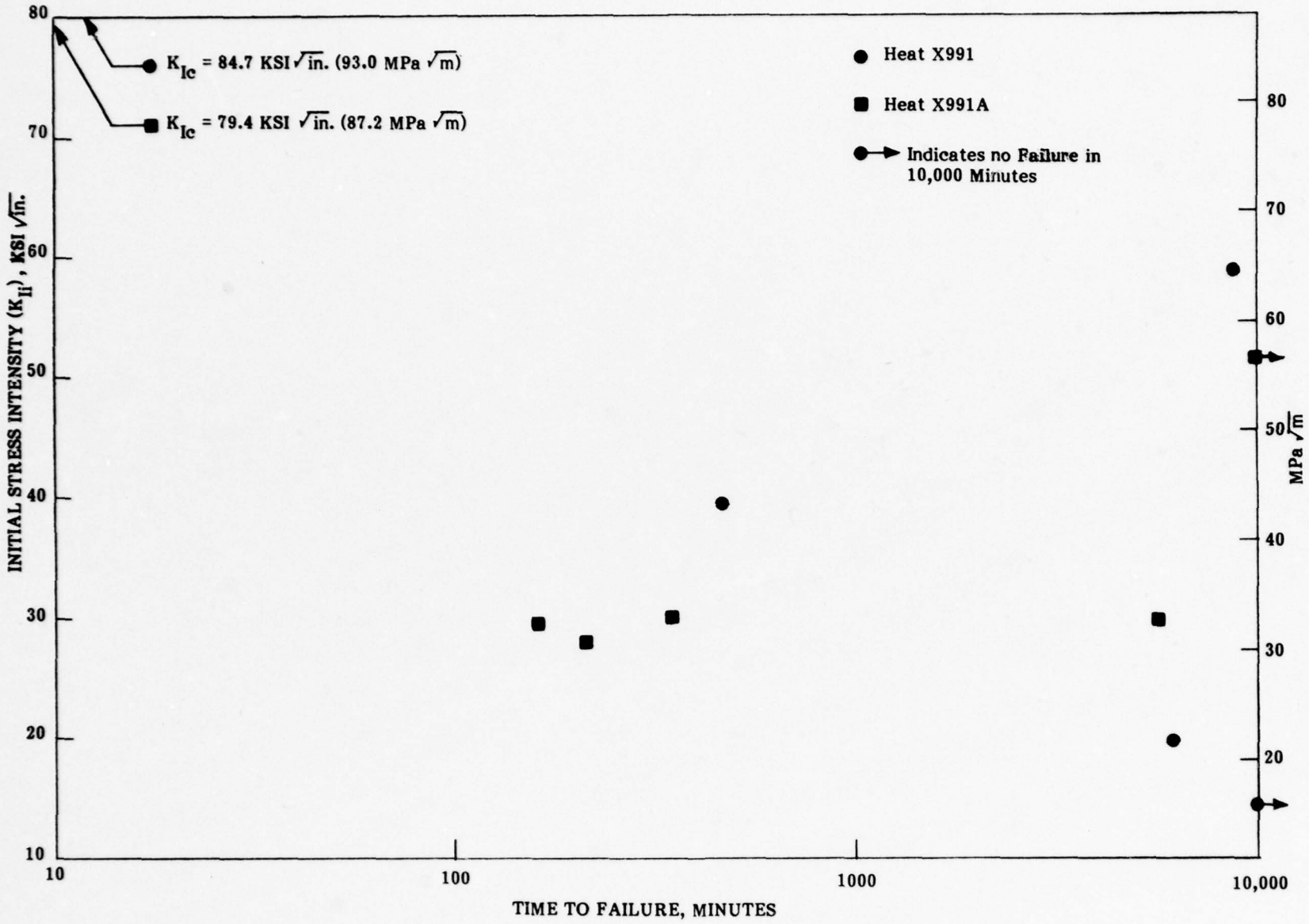

Figure 5. Hydrogen-induced delayed failure time as a function of initial stress intensity for 4340 steel with 0.2% Ce, tempered at 400°F (480°K).

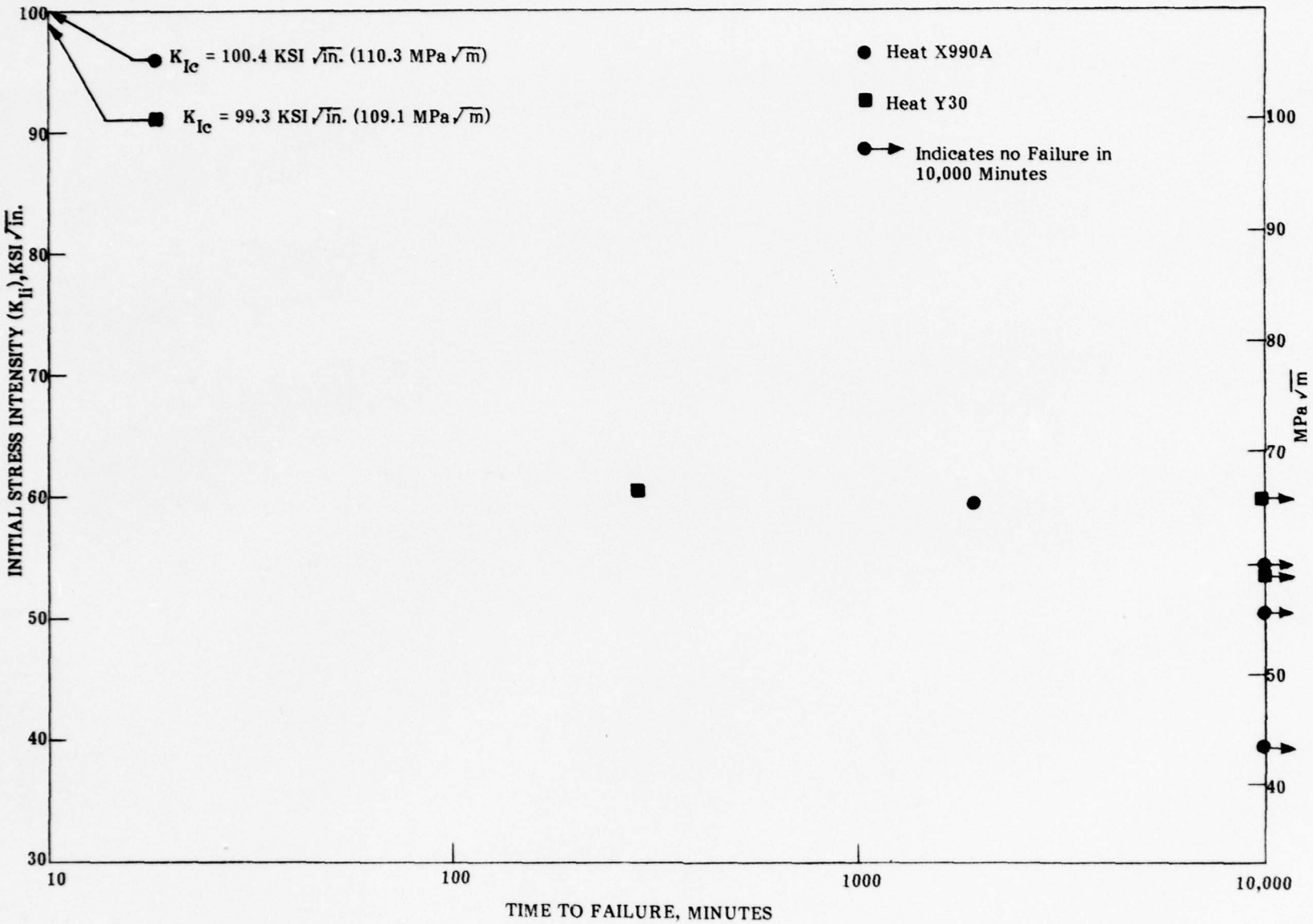

Figure 6. Hydrogen-induced delayed failure time as a function of initial stress intensity for 4340 steel without cerium, tempered at 750°F (670°K).

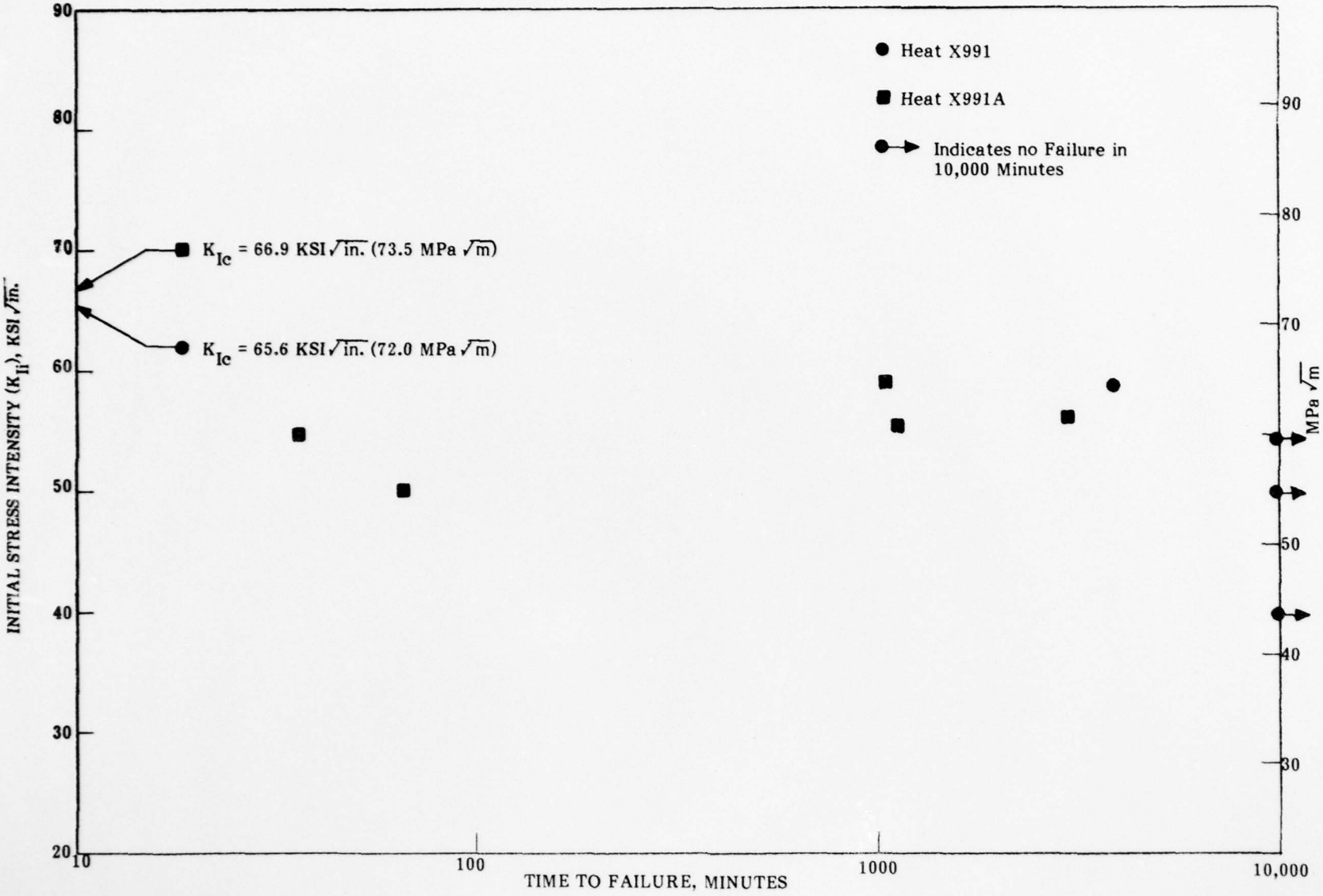

Figure 7. Hydrogen-induced delayed failure time as a function of initial stress intensity for 4340 steel with 0.2% Ce, tempered at 750°F (670°K).

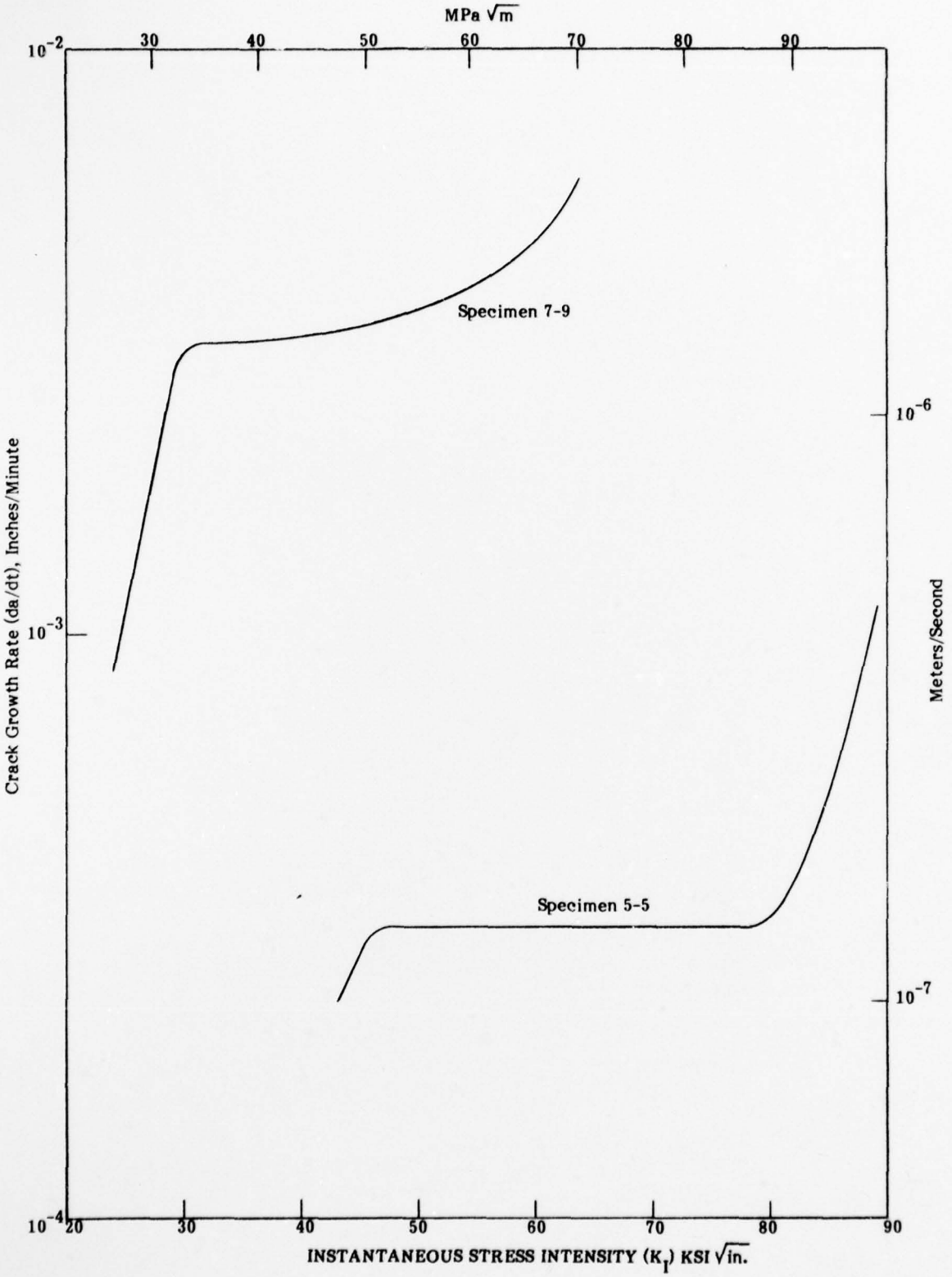

Figure 8. Hydrogen-induced crack growth rate as a function of instantaneous stress intensity for 4340 steel without cerium, tempered at 400°F (480°K).

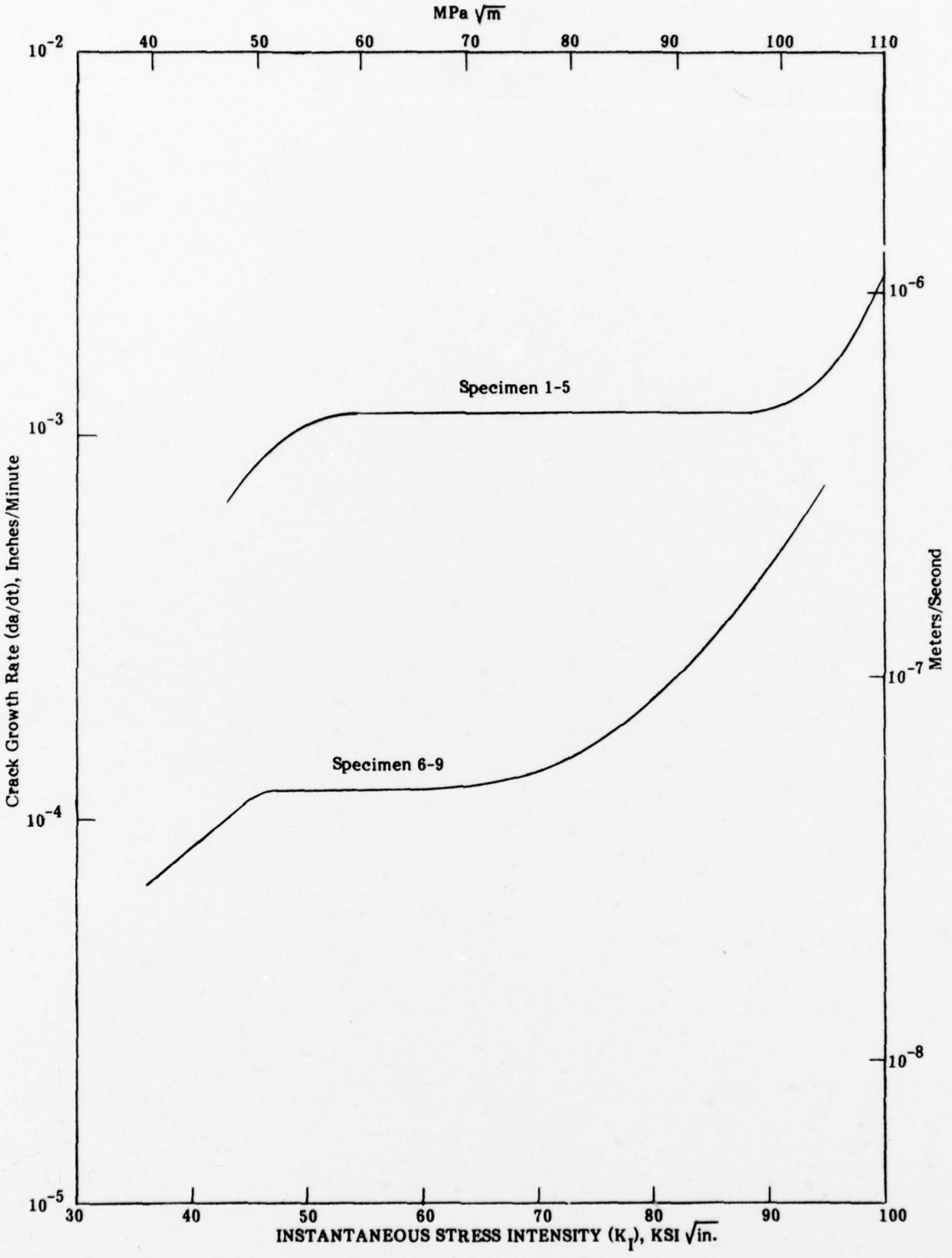

Figure 9. Hydrogen-induced crack growth rate as a function of instantaneous stress intensity for 4340 steel with 0.2% Ce, tempered at 400°F (480°K).

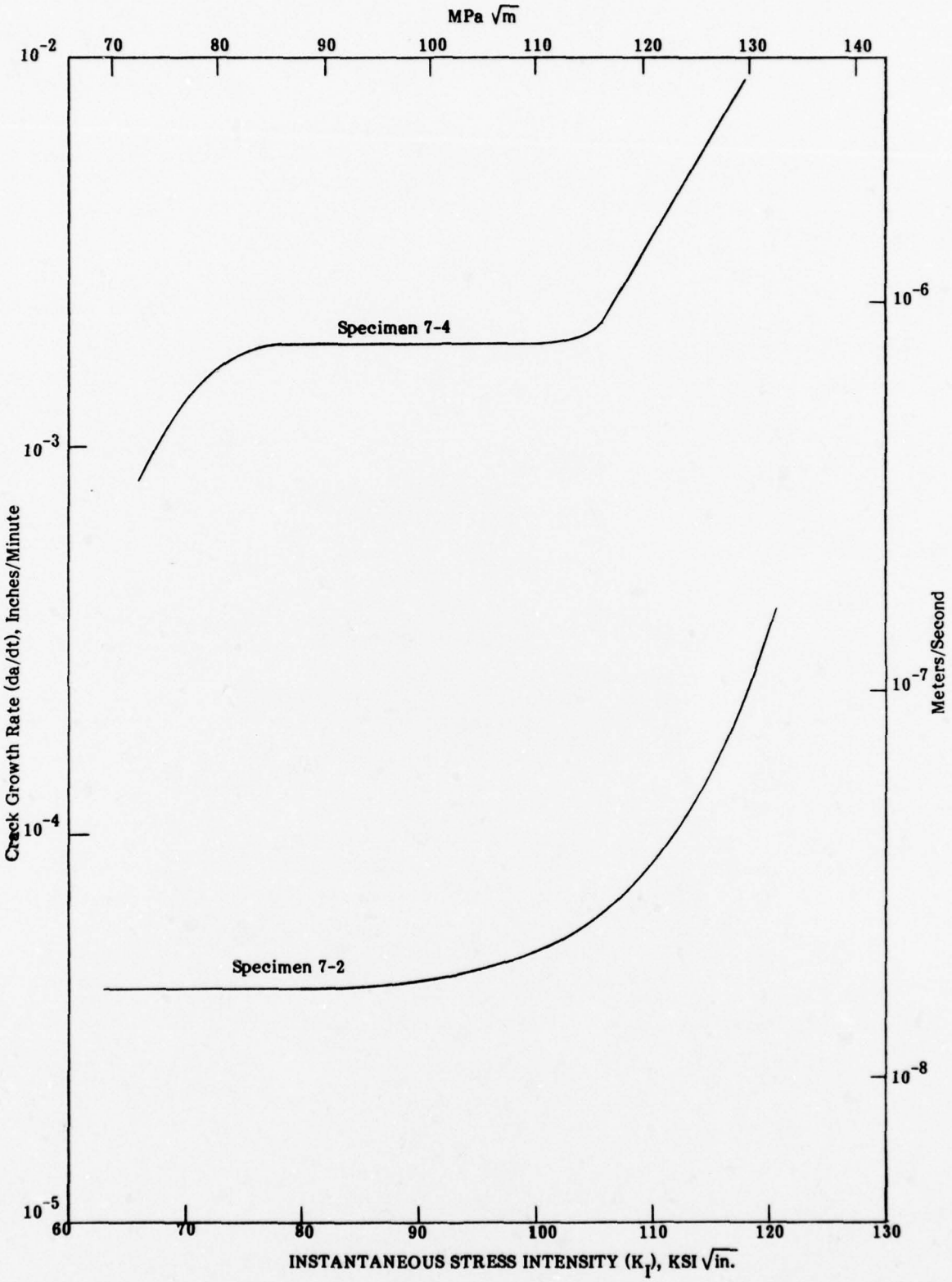

Figure 10. Hydrogen-induced crack growth rate as a function of instantaneous stress intensity for 4340 steel without cerium, tempered at 750°F (670°K).

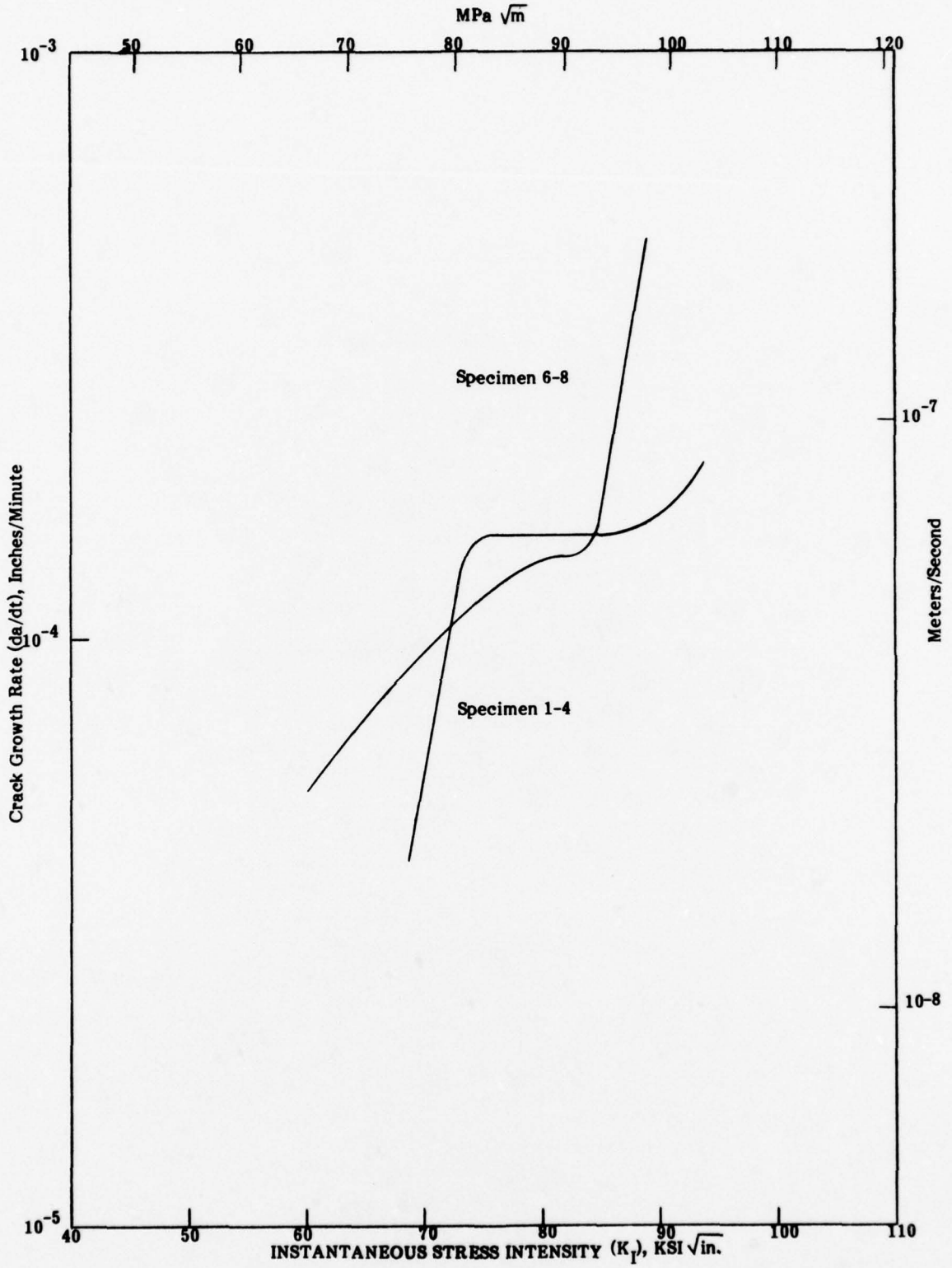

Figure 11. Hydrogen-induced crack growth rate as a function of instantaneous stress intensity for 4340 steel with 0.2% Ce, tempered at 750°F (670°K).

Table 7

Fracture Toughness of 4340 Steel Heats

Specimen Number	Heat Number	Cerium Content %	Fracture Toughness (K_{Ic}) ksi $\sqrt{in.}$	Fracture Toughness (K_{Ic}) MPa $\sqrt{m}$	Remarks
		Tempered at 400°F (480°K)			
5-1	X990A	0	80.2	88.1	
7-1	Y30	0	73.6	80.9	
1-1	X991	0.21	84.7	93.0	Not valid K_{Ic}, excessive plasticity
6-1	X991A	0.20	79.4	87.2	Not valid K_{Ic}, excessive plasticity
		Tempered at 750°F (670°K)			
5-2	X990A	0	100.4	110.3	Not valid K_{Ic}, not plane strain
7-10	Y30	0	99.3	109.1	Not valid K_{Ic}, not plane strain
1-2	X991	0.21	65.6	72.0	
6-2	X991A	0.20	66.9	73.5	

As is evident from Tables 3 through 6 and Figures 4 through 7, there was considerable scatter in the delayed failure data. This variability was attributed to two sources: a loss of hydrogen from the specimens during the storage period between plating and testing, and a nonuniform distribution of cerium in the rare earth modified steel. It was noted that, for a given heat and tempering condition, the failure time at a given K_{Ii} level generally increased with increasing storage time. This occurred both for heats made with and without cerium and at both temper conditions, and is evidenced by the results for specimens 7-7, 7-9, and 7-11 of heat Y30 (Table 3), specimens 6-5, 6-7, and 6-9 of heat X991A (Table 4), and specimens 6-6, 6-8, and 6-10 of heat X991A (Table 6). Hydrogen-induced crack growth in high strength steels is believed to occur by the accumulation of a critical hydrogen concentration at the tip of the crack where the hydrogen locally embrittles the metal (4,5,18). At any given stress intensity level above the hydrogen embrittlement cracking threshold, the rate of crack growth (and hence, the failure time) depends on the rate at which hydrogen is transported to the crack tip, which in turn depends on the hydrogen content in the bulk of the metal. Thus, the observed increase in failure time with increasing storage time suggested that hydrogen had escaped from the specimens during storage so that the hydrogen content was lower in specimens stored for longer periods prior to delayed failure testing. In order to verify this hypothesis, a baking experiment was performed. Since baking accelerates hydrogen movement out of steel (29), baking times longer than the 1 hour employed in the regular specimen preparation should result in longer failure times at the same K_{Ii} level. Thus, specimens 7-2 and 7-12 of heat Y30 were baked at 300°F (420°K) for 10 and 112 hours, respectively, after cadmium plating. Both of these specimens had relatively short storage times (2 and 8 days, respectively). These two specimens were then tested at a K_{Ii} level of approximately 60 ksi $\sqrt{\text{in.}}$ (66 MPa $\sqrt{\text{m}}$) and the results compared with those for specimen 7-4, which was from the same heat, was in the same temper condition, had a similar storage time (3 days) and was tested at about the same K_{Ii} level, but had been given the regular 1-hour baking treatment. As indicated in Table 5, this comparison showed that increasing the baking time from 1 to 10 hours increased the failure time from 288 to 8766 minutes, while a further increase in baking time to 112 hours resulted in no failure in the 10,000 minutes allotted for the delayed failure test. Therefore, some hydrogen was able to escape from the specimens during storage. Examination of the mouth of the crack at the end of the EDM slot, under a binocular microscope, revealed that the cadmium plating did not completely seal the crack opening. Since the cadmium plating was an effective barrier to hydrogen passage through the surface, the path of escape was probably through the mouth of the crack.

The other suspected cause of the large scatter in the delayed failure data, a nonuniform distribution of cerium in the rare earth modified steel, was suggested by the appearance of the fracture surfaces of the specimens. In the previous study of the effect of rare earth additions on the hydrogen embrittlement resistance of 4340 steel (20), many longitudinal ridges were present on the fracture surfaces, both in the hydrogen-induced cracking area and the rapid fracture area, of the compact tension delayed failure specimens of the rare earth modified steels. The number of ridges increased with increasing rare earth content. These ridges were attributed to separation along the rare earth oxide inclusions which were elongated by the forging and hot rolling operations (21). In the present work, it was noted that the number of these ridges on the fracture surfaces of the specimens from the heats containing cerium

varied from specimen to specimen, indicating that the cerium content varied from one specimen to another. This variation probably resulted from inadequate mixing when the cerium was added to the heat. In the previous study (20), little improvement in hydrogen embrittlement resistance occurred for rare earth additions less than about 0.2 weight percent. Therefore, a delayed failure specimen having a lower cerium content in the area of crack growth would behave similar to a specimen from a heat with no rare earths added, which would contribute to the scatter in the delayed failure data.

In addition to delayed failure time, hydrogen embrittlement cracking behavior was characterized in terms of crack growth rate (da/dt) as a function of instantaneous stress intensity factor (K_I) for each test specimen. Representative curves of da/dt versus K_I are shown in Figures 8 through 11. These curves generally exhibit a characteristic shape typical of environment-induced subcritical crack growth under sustained load (1,20). Three stages of da/dt - K_I behavior can be identified. At low K_I levels, da/dt increases rapidly with increasing K_I (Stage I). At intermediate K_I levels, da/dt is either independent of K_I or only slightly K_I-dependent (Stage II). At higher K_I levels, da/dt again increases rapidly with increasing K_I (Stage III). This last stage is followed by rapid fracture of the specimen. Stage II behavior is generally associated with crack growth limited either by mass transport or by the kinetics of a reaction between the metal and its environment. In the present case, the crack growth rate in Stage II is most likely controlled by the diffusion of hydrogen from the bulk of the metal to the tip of the growing crack. The da/dt - K_I curves substantiate the high degree of scatter in the delayed failure data, i.e., in tests for which there was a large difference in failure time, there was also a large difference in crack growth rate at any given K_I level (Figures 8 through 10). This indicates that the scatter in the delayed failure times was not merely due to variability in crack growth incubation time or the K_I level at the onset of rapid fracture, but was associated with variations in the kinetics of crack growth. Thus, the variations in hydrogen content and cerium content from one specimen to another affected the crack growth rate.

Because of the high degree of scatter in the delayed failure test data, no conclusions were drawn regarding the effect of cerium additions on the hydrogen embrittlement cracking resistance of 4340 steel tempered at 400°F (480°K) and 750°F (670°K). However, this work indicated that a uniform distribution of rare earths in the steel is necessary to obtain a consistent benefit from the rare earth additions. Therefore, research is needed to develop a method of incorporating rare earth elements into the microstructure of high strength steels in a more homogeneous distribution.

C. Hydrogen Permeability Results

The results of the hydrogen permeability measurements are presented in Table 8. The half-time to reach the steady state hydrogen permeation flux was determined only at a charging current density of 65 mA/in^2 (1 x 10^5 mA/m^2) because the charging current density on each specimen was successively decreased after the hydrogen permeation flux had reached steady state. The permeation transients at the two subsequent charging current densities would thus be affected by the previous permeation runs in the same specimen. The half-time to reach the steady state hydrogen permeation flux is a relative measure of the apparent hydrogen diffusivity in the metal. This half-time at a charge current density of 65 mA/in^2 (1 x10^5 mA/m^2) was four times longer in the cerium-bearing steel than in the non-cerium steel in the 400°F (480°K) temper condition and 2.5 times longer in the cerium-bearing steel than in the non-cerium steel tempered at 750°F (670°K). These results indicate that the apparent hydrogen diffusivity is lower in the steel containing cerium, at both tempering temperatures. However, because hydrogen permeation transients are affected by hydrogen trapping and surface reactions (27,30,31), it cannot be deduced whether the cerium reduced the true (lattice) hydrogen diffusivity. Cerium compounds in the steel could be potent traps for hydrogen since the rare earth elements are known to combine readily with hydrogen (32). In addition, since most of the cerium in the steel was present as oxide inclusions (20) and solid-solid interfaces are believed to be important sites for hydrogen trapping (31), the inclusion-matrix interface may be a potent hydrogen trap in cerium-bearing 4340 steel. Although the surfaces of the cerium-bearing and non-cerium steel membranes were identically prepared, the electrochemical reactions at the surface of the former could be affected by the presence of the cerium. Thus, hydrogen trapping and changes in surface chemistry may have been responsible for reducing the apparent hydrogen diffusivity of 4340 steel when cerium was added to this alloy.

The results given in Table 8 also show that the steady state hydrogen permeation flux was three to four times lower in the cerium-bearing steel than in the non-cerium steel at both tempering temperatures and all three charging current densities. Since permeability is the product of solubility and diffusivity, the effect of the cerium on the steady state permeation flux could be due to its effect on either or both the hydrogen solubility or the hydrogen diffusivity in the steel. The separate effects of cerium on the solubility and the diffusivity of hydrogen in steels are not presently known, but in view of the strong affinity of the rare earth elements for hydrogen, the solubility would be expected to be increased and the diffusivity decreased by the addition of cerium to steels. Thus, the reduced hydrogen permeability in the cerium-bearing 4340 steel is probably associated with a lower hydrogen diffusivity. The steady state hydrogen permeation flux was not affected by tempering temperature for either the cerium-bearing or the non-cerium steel. This result could be due to constant hydrogen solubility and diffusivity or compensating variations in hydrogen solubility and diffusivity with temperature in this range of tempering temperatures. Hydrogen permeability has been reported to decrease slightly and hydrogen diffusivity to remain constant for a similar high strength steel (British R.S. 140) when the tempering temperature was increased from 400°F (480°K) to 750°F (670°K) (33). In general, it can

Table 8

Hydrogen Permeability Through 4340 Steel

Charging Current Density		Half-Time to Steady State Flux, Minutes		Steady State Hydrogen Permeation Flux			
mA/in^2	mA/m^2			$\mu A/in^2$	$\mu A/m^2$	$\mu A/in^2$	$\mu A/m^2$
		Heat X990A (0% Ce)	Heat X991 (0.2% Ce)	Heat X990A (0% Ce)		Heat X991 (0.2% Ce)	
			Tempered at 400°F (480°K)				
65	1×10^5	30	120	2.17×10^2	3.37×10^5	4.8×10	7.4×10^4
32	5×10^4	-	-	1.33×10^2	2.06×10^5	2.9×10	4.5×10^4
9.7	1.5×10^4	-	-	6.45×10	1.00×10^5	2.3×10	3.5×10^4
			Tempered at 750°F (670° K)				
65	1×10^5	75	190	2.17×10^2	3.37×10^5	5.4×10	8.3×10^4
32	5×10^4	-	-	1.17×10^2	1.81×10^5	4.2×10	6.5×10^4
9.7	1.5×10^4	-	-	6.77×10	1.05×10^5	-	-

be concluded that the presence of cerium retarded the permeability of hydrogen through 4340 steel at both tempering temperatures. Since this would reduce the rate of flow of hydrogen from the bulk of the metal to the tip of the crack, the presence of cerium would be expected to decrease the rate of hydrogen-induced crack growth and increase the delayed failure time in a high strength steel.

IV SUMMARY AND CONCLUSIONS

The addition of the rare earth element cerium to AISI 4340 steel was investigated as a means of inhibiting hydrogen embrittlement cracking in this alloy. Previous work had indicated that rare earth additions at levels of approximately 0.2 weight percent substantially improved the resistance of this steel to hydrogen embrittlement cracking. Because the most important metallurgical variable affecting the susceptibility of high strength steels to hydrogen embrittlement is the strength level of the steel, the effect of cerium additions on the hydrogen embrittlement cracking resistance of 4340 steel was evaluated at two different strength levels. The experimental work included the preparation of four 50-pound (23-kg) heats of 4340 steel, two containing 0.2 weight percent cerium and two with no rare earth elements added, which were vacuum-induction melted and hot worked into plate form. The test material was heat treated to yield strength levels of approximately 210 and 185 ksi (1450 and 1280 MPa). The resistance to hydrogen embrittlement cracking was determined by conducting sustained-load delayed failure tests at room temperature on fatigue-precracked compact tension specimens which were electrolytically charged with hydrogen, plated with cadmium, and baked at 300°F (420°K) for 60 minutes. In addition, hydrogen permeability measurements were made on samples from one of the cerium-bearing heats and one of the non-cerium heats heat treated to both strength levels, to determine whether hydrogen transport through the steel was affected by the presence of the cerium.

The delayed failure results exhibited scatter to the extent that no clear conclusions could be drawn from the data. This scatter was attributed to (1) a loss of hydrogen from the compact tension specimens during the storage period between cadmium plating and testing and (2) a nonuniform distribution of cerium in the rare earth modified steel. It was observed that, for each heat and strength level, the failure time at a given initial stress intensity level generally increased with increasing storage time. Since the hydrogen induced delayed failure time depends on the hydrogen content of the metal, this observation suggested that hydrogen had escaped from the specimens during storage so that the hydrogen content was lower in specimens stored for longer periods prior to delayed failure testing. The path of escape was believed to be through the mouth of the crack since the cadmium plating did not completely seal the crack opening. It was also observed that the number of longitudinal ridges on the fracture surfaces of the delayed failure specimens from the cerium-bearing heats varied from one specimen to another. Since previous work had shown that these ridges were associated with rare earth oxide inclusions and that their number increased with increasing rare earth content, this observation indicated that the cerium content varied from specimen to specimen. Because little improvement in hydrogen embrittlement resistance was found for rare earth additions less than about 0.2 weight percent in the previous study, this variability in the cerium content would contribute to the scatter in the delayed failure data. Because of this scatter, no conclusions were drawn regarding the effect of cerium additions on the hydrogen embrittlement cracking resistance of 4340 steel at the two strength levels.

The hydrogen permeability results showed that the half-time to reach the steady state hydrogen permeation flux at a given charging current density was much longer in the cerium-bearing steel than in the non-cerium steel at both strength levels. These results indicated that the apparent hydrogen diffusivity was lower in the steel containing cerium, at both strength levels. Hydrogen trapping by cerium compounds and changes in surface chemistry were suggested as possible causes for reducing the apparent hydrogen diffusivity of 4340 steel when cerium was added to this alloy. The permeability results also showed that the steady state hydrogen permeation flux at a given charging current density was three to four times lower in the cerium-bearing steel than in the non-cerium steel at both strength levels. The reduced hydrogen permeability in the cerium-bearing steel was probably associated with a lower hydrogen diffusivity in this steel. It was concluded that the presence of cerium retarded the permeability of hydrogen through 4340 steel at both strength levels.

V REFERENCES

1. I. M. Bernstein and A. W. Thompson, eds., Hydrogen in Metals, American Society for Metals, Metals Park, Ohio, 1974.

2. G. R. Pressouyre, "The Role of Trapping on Hydrogen Transport and Embrittlement," Ph.D. Thesis, Carnegie-Mellon University,1977.

3. C. A. Zapffe and C. E. Sims, "Hydrogen, Flakes and Shatter Cracks," Metals and Alloys, Vol. 11, No. 5, 1940, pp. 145-151.

4. A. R. Troiano, "The Role of Hydrogen and Other Interstitials in the Mechanical Behavior of Metals, Trans. ASM, Vol. 52, 1960, pp. 54-80.

5. R. A. Oriani, "A Mechanistic Theory of Hydrogen Embrittlement of Steels," Berichte der Bunsen-Gesellschaft fur Physikalische Chemie, Vol 76, 1972, pp. 848-857.

6. W. M. Cain and A. R. Troiano, "Steel Structure and Hydrogen Embrittlement," Petroleum Engineer, May 1965, pp. 78-82.

7. R. A. McCoy, "Development of a High-Strength Manganese Steel Resistant to Hydrogen Embrittlement," Hydrogen in Metals, I. M. Bernstein and A. W. Thompson, eds., American Society for Metals, 1974, pp. 169-182.

8. I. M. Bernstein and A. W. Thompson, "Effect of Metallurgical Variables on Environmental Fracture of Steels," Intl. Metals Reviews, December 1976, pp. 269-287.

9. H. H. Johnson, J. G. Morlet, and A. R. Troiano, "Hydrogen, Crack Initiation, and Delayed Failure in Steel," Trans. AIME, Vol. 212, August 1978. pp. 528-536.

10. W. Beck and E. J. Jankowsky, "Effects of Plating High Tensile Strength Steels," Proc. American Electroplaters Society, Vol. 44, 1957, pp. 47-52.

11. W. Beck and E. J. Jankowsky, "The Effectiveness of Metallic Undercoats in Minimizing Plating Embrittlement of Ultra High Strength Steel," Proc. American Electroplaters Society, Vol. 47, 1960, pp. 152-159.

12. L. H. McEowan and A. R. Elsea, "Behavior of High Strength Steels under Cathodic Protection," Corrosion, Vo. 21, 1965, pp. 28-37.

13. F. N. Speller, Corrosion, Causes and Prevention, 3rd Edition, McGraw-Hill, New York, 1951, pp. 320-376.

14. R. P. Wei and G. W. Simmons, "Environment Enhanced Fatigue Crack Growth in High-Strength Steels," Technical Report No. 1, Contract N00014-67-A-03700008, NR 036-097, March 1973.

15. H. W. Liu, Ya-lung Hu, and P. J. Ficalora, "The Control of Catalytic Poisoning and Stress Corrosion Cracking," Eng. Fracture Mech., Vol. 5, No. 2, June 1973, pp. 281-292.

16. E. I. Nikolaev, Yu., V. Kryakovskii, E. I. Tyurin, and V. I. Yanoiskii, "Chemical Heterogeneity and Nonmetallic Inclusions in Steel Ingots Containing Rare Earth Metals," Izv., VUZ - Chern. Met., 1965 (7), pp. 37-42; English translation, H. Brutcher, No. 6626.

17. H. Homma, "A Study of Delayed Cracking in HY-80 Weldments," Ph.D. Thesis, Rensselaer Polytechnic Institute, 1973.

18. W. F. Savage, "The Effect of Rare Earth Additions on Hydrogen-Induced Cracking in HY-80 Weldments," Presented at the International Symposium on Sulfide Inclusions in Steel, 7-8 November 1974, Port Chester, New York.

19. D. G. Howden and P. A. Tewa, "Hydrogen in HY-130 Weld Metal," Battelle Columbus Laboratories report prepared for ONR Contract No. N00014-74-C-0407, NR 031770, July 31, 1975.

20. C. S. Kortovich, "Inhibition of Hydrogen Embrittlement in High Strength Steel," TRW Technical Report No. ER-7814-2, prepared for ONR Contract No. N00014-74-C-0365, February 1977.

21. A. A. Sheinker, "Effect of Rare Earth Additions on Stress Corrosion Cracking of 4340 Steel," TRW Technical Report No. ER-7814-3, Prepared for ONR Contract No. N00014-74-C-0365, Januaray 1978.

22. C. S. Carter, "The Effect of Silicon on the Stress Corrosion Resistance of Low Alloy High Strength Steels," Corrosion, Vol. 25, No. 10, October 1969, pp. 423-431.

23. C. F. Barth and E. A. Steigerwald, "Evaluation of Hydrogen Embrittlement Mechanisms," Met. Trans., Vol. 1, December 1970, pp. 3451-3455.

24. "Standard Test Method for Plane-Strain Fracture Toughness of Metallic Materials," ASTM E 399-74, 1977 Annual Book of ASTM Standards, Part 10, American Society for Testing and Materials, Philadelphia, 1977, pp. 505-524.

25. A. Saxena and S. J. Hudak, Jr. "Review and Extension of Compliance Information for Common Crack Growth Specimens," Intl. Journal of Fracture, to be published.

26. M.A.V. Devanathan and Z.O.J. Stachurski, "The Absorption and Diffusion of Electrolytic Hydrogen in Palladium," Proc. of the Royal Society, Vol. A270, 1962, p. 90.

27. S. S. Chatterjee, B. G. Ateya, and H. W. Pickering, "Effect of Electrodeposited Metals on the Permeation of Hydrogen Through Iron Membranes," Met. Trans. A, Vol. 9A, March 1978, pp. 389-395.

28. W. W. Gerberich and Y. T. Chen, "Hydrogen-Controlled Cracking - An Approach to Threshold Stress Intensity," Met. Trans. A, Vol. 6A, No. 2, February 1975, pp. 271-278.

29. H. H. Johnson, J. G. Morlet, and A. R. Troiano, "Hydrogen, Crack Initiation, and Delayed Failure in Steel," Trans. AIME, Vol. 212, August 1978, pp. 528-536.

30. R. A. Oriani, "Hydrogen in Metals," Fundamental Aspects of Stress Corrosion Cracking, R. W. Staehle, A. J. Forty, and D. van Rooyen, eds., National Association of Corrosion Engineers, Houston, 1969, pp. 32-49.

31. R. A. Oriani, "The Diffusion and Trapping of Hydrogen in Steel," Acta Met., Vol. 18, January 1970, pp. 147-157.

32. K. A. Gschneidner, Jr., Rare Earth Alloys, D. Van Nostrand Co., Princeton, N.J., 1961.

33. T. P. Radhakrishnan and L. L. Schreir, "Hydrogen Permeation Through Iron and Steel by Electrochemical Transfer - II. Influence of Metallurgical Factors on Hydrogen Permeation," Electrochimica Acta, Vol. 12, 1967, pp. 889-903.

BASIC DISTRIBUTION LIST

Technical and Summary Reports

Organization	Copies
Defense Documentation Center Cameron Station Alexandria, Virginia 22314	12
Office of Naval Research Department of the Navy 800 N. Quincy Street Arlington, Virginia 22217	
Attention: Code 471	1
Code 102	1
Code 470	1
Commanding Officer Office of Naval Research Branch Office Building 114, Section D 666 Summer Street Boston, Massachusetts 02210	1
Commanding Officer Office of Naval Research Branch Office 536 South Clark Street Chicago, Illinois 60605	1
Office of Naval Research San Francisco Area Office 760 Market Street, Room 447 San Francisco, California 94102	1
Naval Research Laboratory Washington, D.C. 20375	
Attention: Codes 6000	1
6100	1
6300	1
6400	1
2627	1
Naval Air Development Center Code 302 Warminster, Pennsylvania 18964 Attention: Mr. F. S. Williams	1
Naval Air Propulsion Test Center Trenton, New Jersey 08628 Attention: Library	1
Naval Construction Batallion Civil Engineering Laboratory Port Hueneme, California 93043 Attention: Materials Division	1
Naval Electronics Laboratory San Diego, California 92152 Attention: Electron Materials Sciences Division	1
Naval Missile Center Materials Consultant Code 3312-1 Point Mugu, California 92041	1
Commanding Officer Naval Surface Weapons Center White Oak Laboratory Silver Spring, Maryland 20910 Attention: Library	1
David W. Taylor Naval Ship Research and Development Center Materials Department Annapolis, Maryland 21402	1
Naval Undersea Center San Diego, California 92132 Attention: Library	1
Naval Underwater System Center Newport, Rhode Island 02840 Attention: Library	1
Naval Weapons Center China Lake, California 93555 Attention: Library	1
Naval Postgraduate School Monterey, California 93940 Attention: Mechanical Engineering Department	1

Organization	Copies
Naval Air Systems Command Washington, D.C. 20360 Attention: Codes 52031 52032	1
Naval Sea System Command Washington, D.C. 20362 Attention: Code 035	1
Nval Facilities Engineering Command Alexandria, Virginia 22331 Attention: Code 03	1
Scientific Advisor Commandant of the Marine Corps Washington, D.C. 20380 Attention: Code AX	1
Naval Ship Engineering Center Department of the Navy Washington, D.C. 20360 Attention: Code 6101	1
Army Research Office P.O. Box 12211 Triangle Park, North Carolina 27709 Attention: Metallurgy & Ceramics Program	1
Army Materials and Mechanics Research Center Watertown, Massachussetts 02172 Attention: Research Programs Office	1
Air Force Office of Scientific Research Building 410 Bolling Air Force Base Washington, D.C. 20332 Attn: Chemical Science Directorate Electronics & Solid State Sciences Directorate	1 1
Air Force Materials Laboratory Wright-Patterson Air Force Base Dayton, Ohio 45433	1
Library Building 50, Room 134 Lawrence Radiation Laboratory Berkely, California	1
NASA Headquarters Washington, D.C. 20546 Attention: Code RRM	1
NASA Lewis Research Center 21000 Brookpark Road Cleveland, Ohio 44135 Attention: Library	1
National Bureau of Standards Washington, D.C. 20234 Attention: Metallurgy Division Inorganic Materials Div.	1 1
Director Applied Physics Laboratory University of Washington 1013 Northeast Fortieth Street Seattle, Washington 98105	1
Defense Metals and Ceramics Information Center Battelle Memorial Institute 505 King Avenue Columbus, Ohio 43201	1
Metals and Ceramics Division Oak Ridge National Laboratory P.O. Box X Oak Ridge, Tennessee 37380	1
Los Alamos Scientific Laboratory P.O. Box 1663 Los Alamos, New Mexico 87544 Attention: Report Librarian	1
Argonne National Laboratory Metallurgy Division P.O. Box 229 Lemont, Illinois 60439	1
Brookhaven National Laboratory Technical Information Division Upton, Long Island New York 11973 Attention: Research Library	1
Office of Naval Research Branch Office 1030 East Green Street Pasadena, California 91106	1

SUPPLEMENTARY DISTRIBUTION LIST

Technical and Summary Reports

Professor G. S. Ansell
Rensselaer Polytechnic Institute
Department of Metallurgical Engineering
Troy, New York 12181

Professor H. K. Birnbaum
University of Illinois
Department of Metallurgy
Urbana, Illinois 61801

Dr. E. M. Breinan
United Aircraft Corporation
United Aircraft Research Labortories
East Hartford, Connecticut 06108

Professor H. D. Brody
University of Pittsburgh
School of Engineering
Pittsburgh, Pennsylvania 14213

Mr. P. J. Cacciatore
General Dynamics
Electric Boat Division
Eastern Point Road
Groton, Connecticut 06340

Professor J. B. Cohen
Northwestern University
Department of Material Sciences
Evanston, Illinois 60201

Professor M. Cohen
Massachusetts Institute of Technology
Department of Metallurgy
Cambridge, Massachusetts 02139

Professor Thomas W. Eagar
Massachusetts Institute of Technology
Department of Materials
Science and Engineering
Cambridge, Massachusetts 02139

Professor B. C. Giessen
Northeastern University
Department of Chemistry
Boston, Massachusetts 02115

Dr. G. T. Hahn
Battelle Memorial Institute
Department of Metallurgy
505 King Avenue
Columbus, Ohio 43201

Professor D. G. Howden
Ohio State University
Dept. of Welding Engineering
190 West 19th Avenue
Columbus, Ohio 43210

Dr. C. S. Kortovich
TRW Inc.
23555 Euclid Avenue
Cleveland, OHio 44117

Professor D. A. Koss
Michigan Technological University
College of Engineering
Houghton, Michigan 49931

Professor A. Lawley
Drexel University
Dept. of Metallurgical Engineering
Philadelphia, Pennsylvania 19104

Professor Harris Marcus
The University of Texas at Austin
College of Engineering
Austin, Texas 78712

Dr. H. Margolin
Polytechnic Institute of New York
333 Jay Street
Brooklyn, New York 11201

Professor K. Masubuchi
Massachusetts Institute of Technology
Department of Ocean Engineering
Cambridge, Massachusetts 02139

Dr. H. I. McHenry
National Bureau of Standards
Institute for Basic Standards
Boulder, Colorado 80302

Professor J. W. Morris, Jr.
University of California
College of Engineering
Berkeley, California 94720

Professor Ono
University of California
Materials Department
Los Angeles, California 90024

Dr. Neil E. Paton
Rockwell International
Science Center
1049 Camino Dos Rios
P.O. Box 1085
Thousand Oaks, California 91360

Mr. A. Pollack
Naval Ships Reserach & Development
Center
Annapolis, Maryland 21402

Dr. Karl M. Prewo
United Technologies Laboratories
United Technologies Corporation
East Hartford, Conecticut 06108

Professor W. F. Savage
Rensselaer Polytechnic Institute
School of Engineering
Troy, New York 12181

Professor O. D. Sherby
Stanford University
Materials Sciences Division
Stanford, California 94300

Professor J. Shyne
Stanford University
Materials Sciences Division
Stanford, California 94300

Dr. R. P. Simpson
Westingshouse Electric Corporation
Research & Development Center
Pittsburgh, Pennsylvania 15235

Dr. E. A. Starke, Jr.
Georgia Institute of Technology
School of Chemical Engineering
Atlanta, Georgia 30332

Professor David Turnbull
Harvard University
Division of Engineering & Applied
Physics
Cambridge, Massachusetts 02139

Dr. F. E. Wawner
University of Virginia
School of Enginnering & Applied
Science
Charlottesville, Virginia 22901

Dr. C. R. Whitsett
McDonnell Douglas Research
McDonnell Douglas Corporation
Saint Louis, Missouri 63166

Dr. J. C. Williams
Carnegie-Mellon University
Department of Metallurgy &
Materials Sciences
Schenley Park
Pittsburgh, Pennsylvania 15213

Professor H.G.F. Wilsdorf
University of Virginia
Charlottesville, Virginia 22903

Dr. M. A. Wright
University of Tennessee
Space Institute
Tullahoma, Tennessee 37388